

Efficient All-Optical Helicity-Dependent Switching in Pt/Co/Pt with Dual Laser Pulses

Kihiro T. Yamada^{1,†,*}, Kiran Horabail Prabhakara^{1,†}, Tian Li², Fuyuki Ando², Sergey Semin¹, Teruo Ono^{2,3}, Andrei Kirilyuk^{1,4}, Alexey V. Kimel^{1,*}, Theo Rasing^{1,*}

¹*Radboud University, Institute for Molecules and Materials, 6525 AJ Nijmegen, The Netherlands*

²*Institute for Chemical Research, Kyoto University, Uji, Kyoto 611-0011, Japan.*

³*Center for Spintronics Research Network (CSRN), Graduate School of Engineering Science, Osaka University*

⁴*FELIX Laboratory, Radboud University, Toernooiveld 7c, 6525 ED Nijmegen, The Netherlands*

†These authors contributed equally to this work.

*Corresponding author: k.yamada@science.ru.nl; a.kimel@science.ru.nl; th.rasing@science.ru.nl

All-optical helicity-dependent switching (AO-HDS) in ferromagnetic metals so far requires at least 10^2 - 10^3 laser pulses for fully switching their magnetic states. We demonstrate that using a combination of a short, 90-fs linearly polarized pulse and a subsequent longer, 3-ps circularly polarized pulse can reduce the number of pulses for full switching to 4 pulse pairs in a single stack of Pt/Co/Pt. Dual-pulse AO-HDS proceeds via helicity-independent stochastic nucleation of switched domains and subsequent deterministic helicity-dependent domain wall motion. The ultrafast decrease of the magnetic properties triggered by the short pulse plays a key role in dual-pulse AO-HDS. The obtained results suggest that the dual-pulse approach is a potential route towards realizing efficient AO-HDS in ferromagnetic metals.

The explosive growth of big data and artificial intelligence demands faster and more energy efficient ways to manipulate and store data [1]. One approach is to use current-induced torques to switch magnetization, as in spin-transfer torque magnetic random access memory [2]. Another potential route is to utilize an ultrashort laser pulse [3]. It was demonstrated that in ferrimagnetic transition metal-rare earth alloys [4-6], a single ultrashort laser pulse can switch the magnetization. Furthermore, all-optical helicity-dependent switching (AO-HDS) was recently demonstrated in a variety of ferromagnetic metals, including thin films of Co/Pt [7-12] and Co/Ni [9], as well as granular alloys with high coercivity, like CoAgPt [7] and FePt [13]. It is now widely accepted that the switching proceeds via two stages: helicity-independent stochastic nucleation of switched domains and helicity-dependent deterministic domain wall (DW) motion [8, 10-12]. However, the magnetization reversal from fully “up” to fully “down” requires at least 10^2 - 10^3 light pulses [7-13].

In this Letter, we demonstrate a dual-pulse method, schematically shown in Fig.1, to realize efficient AO-HDS in a single stack of Pt/Co/Pt with perpendicular magnetic anisotropy. The first short pulse is used to reduce the magnetization and to nucleate reversed domains and the second circularly polarized pulse coming after a constant time separation can efficiently switch the magnetization by enlarging the reversed nuclei. Indeed, we find that 4 pairs of pulses can fully switch the magnetization, when a 90-fs linearly polarized pulse, acting as the first optical pump for demagnetization, and a subsequent 3-ps circularly polarized pulse, acting as the second optical pump for switching, are used with a pulse interval of 5 ps. In stark contrast, using only circularly polarized pulses, 100 - 150 pulses are still required for fully switching the same stack. Dual-pulse AO-HDS strongly depends on the pulse interval and the pulse width of the circularly polarized pulse. We suggest that the giant heat gradient across DWs induced by the helicity dependent absorption via magnetic circular dichroism can move these DWs, resulting in the very efficient switching with the dual pulse approach.

We used a Pt/Co/Pt stack, which is a typical candidate for spintronic devices [2] as well as for AO-HDS [7-12]. The multilayer of Ta(4 nm)/Pt(3.0 nm)/Co(0.6 nm)/Pt(3.0 nm)/MgO(2.0 nm)/Ta(1.0 nm) was sputtered on a synthetic quartz glass substrate. DC and RF sources were used for depositing Ta, Pt and Co, and MgO, respectively. The MgO/Ta capping layer prevents the magnetic layer from oxidization. The multilayer exhibits a perpendicular easy axis of magnetization as seen from the perfectly square magnetic hysteresis as a function of perpendicular magnetic field (see Fig. S1 in Supplemental Material [14]).

For optical excitation we used a Ti:sapphire amplified laser system (Solstice Ace, Spectra-Physics) of which the central wavelength and repetition rate were 800 nm and 1 KHz, respectively. The amplifier system contains two compressors which allowed independent control of the pulse width for the two pump beams. The laser amplifier was used in external trigger mode, in which with the help of a delay generator (DG645, Stanford Research) we can control the amount of pulses reaching the sample. To detect the magnetic state, magneto-optical Faraday imaging with a white light source as probe was employed as depicted in Fig. S2 [14]. The first linearly polarized pump pulse had a width, τ_{π} , of 90 fs while the second, circularly polarized pump pulse, had a variable width, τ_{σ} , in the range of 0.5 – 3.0 ps and arrived after an adjustable time interval, Δt . The laser pulses had a Gaussian intensity distribution and both were incident at an angle of 15 deg. from the sample normal. The focused beam sizes ($1/e^2$ radius) for the pump pulses were calculated based on the Liu-method [15] (see Supplemental Note 3 [14]). The laser fluence was calculated using the $1/e^2$ radius, the repetition rate (1 kHz), and the average power measured with a power meter. The pump intensity was controlled using a combination of a half wave plate and a Gran-Taylor prism. To achieve precise intensity control of the circularly-polarized pump, the half wave plate was mounted on a motorized stage. A quarter wave plate was placed after the Gran-Taylor prism to convert the linearly polarized beam to a circularly polarized one for the second pump. The probe light from the white light source was linearly polarized by a sheet

polarizer. It was then collimated and incident on the sample surface using a combination of lenses. The transmitted light from the sample was collected by an objective with a magnification of 20 \times . An analyzer, with the polarization axis orthogonal to the polarization of the incident probe light, was placed before a charge-coupled device camera.

Figure 2(a) shows magneto-optical images taken after the film in down(M^-)/up(M^+)-magnetized state was excited with 1,000 right(σ^+)/left(σ^-) circularly polarized light pulses, at a repetition rate of 1 kHz. In the experiment, the pulse width τ_σ was varied in the range of 0.5 – 3.0 ps. Uniform AO-HDS is observed for τ_σ in the range of 1.0 – 3.0 ps. However, a slight increase in fluence F_σ results in a multi-domain structure at the spot center. This is due to a larger demagnetized area in comparison to the equilibrium domain size. Figure 2(b) shows the averaged net magnetization $\langle M \rangle$ after illumination with the laser pulses, as a function of τ_σ and F_σ . $\langle M \rangle$ was determined by averaging the intensity of a 15- μm diameter area (within the excited region) and normalizing it to the corresponding intensity when the magnetic state of the same area was fully switched. The $\langle M \rangle$ diagram indicates that a longer pulse width is more suitable for AO-HDS, as already demonstrated by R. Medapalli et al.[10]. In order to better understand the switching process, snapshots were taken before and after pumping the sample with 150 - 800 circularly polarized pulses ($\tau_\sigma = 3.0$ ps), as shown in Fig. 2(c). It was observed that a few hundred pulses nucleate a switched magnetic domain at the spot center. Subsequent illumination with the pump pulses only increased the switched area by inducing DW motion. Hence, as depicted in Fig. 2(d), the switching process can be separated into (i) nucleation of a switched domain and a (ii) subsequent DW propagation.

In the next set of experiments, we demonstrate that a dual-pulse method is much more efficient for AO-HDS. Figure 3(a) shows snapshots before and after irradiating the sample with 1-5 pair(s) of pulses. Here, the pulse width $\tau_{\pi 1}$ and fluence $F_{\pi 1}$ of the first linearly polarized pulse were fixed at 90 fs and 2.29 mJ/cm², respectively, corresponding to the demagnetization threshold. The

second light pulse with circularly polarization ($\tau_{\sigma 2} = 3.0$ ps and $F_{\sigma 2} = 1.94$ mJ/cm²) was made to reach the sample after a pulse interval $\Delta t = 5.0$ ps. Remarkably, 4 such pulse pairs are sufficient to fully switch the magnetization of a 15- μ m diameter area. This indicates that the dual-pulse method is extremely efficient and a potential approach towards ultrafast AO-HDS in ferromagnetic metals. Dual-pulse AO-HDS with shorter $\tau_{\sigma 2}$ is shown in the Supplemental Material, which also shows that longer pulses are more suitable for dual AO-HDS than shorter ones. Note that a total of 8 pulses is a record small number amongst the existing reports on AO-HDS in ferromagnetic metals [7-13], where at least 10^2 - 10^3 light pulses are required for full switching. For comparison, we display the images obtained for multi-pulse excitations with circularly polarized light ($\tau_{\sigma} = 3.0$ ps and $F_{\sigma} = 5.48$ mJ/cm²) in Fig. 3(b), where the pulse interval between each pulse was set to be at least 1 second. We observed that 100-150 pulses are still required for switching the same area, in contrast to the dual-pulse approach. The required laser fluence increases with decreasing the repetition rate, because the magnetic properties reduce by the accumulated heat in the substrate at high repetition rates [10]. The total laser fluence for full switching with the dual-pulse method, $4 \times (F_{\sigma 1} + F_{\sigma 2}) \sim 17$ mJ/cm², is much smaller than $100 \times F_{\sigma} \sim 548$ mJ/cm² used for the multi-pulse approach. This indicates that the dual-pulse method not only minimizes the number of pulses, but also dramatically reduces the net laser fluence required for switching.

To elucidate the roles of each pulse, we also used circular polarization for the first short pulse as well. Figure 4 shows snapshots taken before and after the sample was pumped with 1-5 pair(s) of short and long circularly polarized pulses. Here, the pulse parameters of the two pulses are as follows: $\tau_{\sigma 1} = 90$ fs, $F_{\sigma 1} = 1.94$ mJ/cm², $\tau_{\sigma 2} = 3.0$ ps, and $F_{\sigma 2} = 1.32$ mJ/cm². The interval between the two pulses was fixed at $\Delta t = 5.0$ ps. Changing the helicity of the first short circularly polarized pulse does not make a clear difference in the switching of the magnetic state. On the other hand, the helicity of the subsequent longer pulse determines whether the magnetic state switches. These results suggest that dual-pulse AO-HDS proceeds via helicity-independent

demagnetization and subsequent helicity-dependent deterministic DW motion, similar as in multi-pulse AO-HDS [8, 10-12].

Because the demagnetization triggered by the short pulse is ultrafast (see Fig. S7 [14]), Δt is considered to be a crucial parameter for dual-pulse AO-HDS. Figure 4(a) shows snapshots taken after illuminating the uniformly magnetized film with 4 dual pulses at positive as well as negative Δt . Here, we used the following laser parameters of the linearly and circularly polarized pulses: $\tau_{\pi} = 90$ fs, $F_{\pi} = 2.35$ mJ/cm², $\tau_{\sigma} = 3.0$ ps, and $F_{\sigma} = 1.26$ mJ/cm². Furthermore, the averaged net magnetization $\langle M \rangle$ after 4 pairs of pulses is plotted in Fig. 4(b) as a function of Δt . $\langle M \rangle$ was determined in the same manner as in the previous section. When the circularly polarized pulse reaches the film before the linearly polarized pulse ($\Delta t < 0.0$ ps), a multi-domain state is stabilized ($\langle M \rangle \sim 0.0$) because the linearly polarized pulse has demagnetized the magnetic state. When the two pulses simultaneously arrive at the film ($\Delta t = 0.0$ ps), the multi-domain area reaches a maximum size. With increasing Δt beyond 0.0 ps, the multi-domain area shrinks and a uniformly switched area appears near the outmost DW; eventually, the multi-domain area disappears and $\langle M \rangle$ gets to -1.0 at around $\Delta t = 5.0$ ps. A further increase in Δt drastically decreases the switched area and increases $\langle M \rangle$. These observations indicate that the ultrafast reduction of the magnetic properties triggered by the first short pulse, the pulse interval and the order of the two pulses are crucial for dual-pulse AO-HDS.

The first important question is: what is the driving force behind AO-HDS in ferromagnetic metals? The obtained results show a clear light helicity dependence of the switching process. This means that the circularly polarized light breaks the degeneracy between two domains with opposite magnetization orientations. Therefore, the effect of the pulse can be expressed in the form of an effective magnetic field. Quantum mechanical treatment of the inverse Faraday effect [16] showed that, next to a relatively small magnetic polarization, a light pulse induces an effective Zeeman field. The peak amplitude of the effective Zeeman field is proportional to the square of the laser

electric field in the system; for instance, stretching the pulse width from 90 fs to 3.0 ps reduces the peak amplitude to 3.0 % at a constant fluence. Since the life time of the photo-excited electrons in Co is short (less than 2 fs at 1.55 eV [17]) with respect to the pulse duration, an increase in pulse duration will significantly decrease the strength of this opto-magnetic phenomenon. Therefore, the inverse Faraday effect is an unlikely candidate to explain the result that the longer pulse is more suitable for AO-HDS in the present system.

Magnetic circularly dichroism (MCD) can produce a heat gradient across a DW, and subsequently push a DW from the hotter (lower DW energy) to the colder (higher DW energy) area [8-12], as the up (down)-magnetized domain absorbs the left (right) circularly polarized light more than the down (up)- magnetized domain. During the cooling process, the DW does not move back to the initial position due to pinning. When a circularly polarized pulse with $F_{\sigma} = 5.48 \text{ mJ/cm}^2$ illuminates the Pt/Co/Pt stack, the heat gradient across a DW is estimated to be $\nabla T = (\Delta A_{\text{MCD}} F_{\sigma}^*) / [w_{\text{DW}} C (t_{\text{Co}} + t_{\text{Pt}})] = 1.7 \text{ K/nm}$. Here, we used an absorbed fluence F_{σ}^* of 2.20 mJ/cm^2 , a typical DW width $w_{\text{DW}} = 10 \text{ nm}$, an MCD coefficient [9] $\Delta A_{\text{MCD}} = 0.015$, a weighted heat capacity [18] $C = 2.93 \text{ MJ/Km}^3$, a Co thickness $t_{\text{Co}} = 0.6 \text{ nm}$, and a Pt thickness $t_{\text{Pt}} = 6.0 \text{ nm}$, respectively. F_{σ}^* was calculated using the complex refractive indices [18] of Co ($2.97 + 4.87i$) and Pt ($2.84 + 4.96i$) at the wavelength of 800 nm and the thickness values given above. This heat gradient across a DW produced by the illumination of the circularly polarized pulse is five orders of magnitude larger than when using conventional heaters [19] to produce a lateral heat gradient. This giant heat gradient can also generate a large spin transfer torque [20-22] to move the DW. Note that it is clear that the temperature gradient increases with increasing the total energy of the laser pulse, apart from the detailed mechanism. Therefore, the longer pulse can supply larger energy to the system without demagnetizing [23] and thus should be more suitable for AO-HDS under this scenario.

The second important question is: why is the dual-pulse method more efficient than the multi-pulse method? Ultrafast demagnetization triggered by the first pulse is crucial to explain this. Just after the arrival of the first short pulse, the magnetization drastically decreases on a time scale of hundreds of femtoseconds (see Refs. [23-27] and Fig. S7 [14]). When the fluence of the short pulse reaches the critical level at which the electron temperature reaches the Curie temperature (T_C), a paramagnetic-like state appears [26, 27]. A switched domain is indeed observed at the center of the spot when using only the short linearly polarized pulse at the demagnetization threshold (see Fig. S4 [14]). Therefore, the fluence of the first pulse was high enough to create a paramagnetic-like state around the center of the spot. After the paramagnetic-like state, small switched domains nucleate stochastically. Subsequently, each domain absorbs an amount of energy from the second longer pulse, depending on its magnetic orientation and the light helicity. The thus formed heat gradients across the DWs move them. The cooler domains expand and merge to form larger domains, whereas the hotter domains shrink and disappear. The helicity of the first short pulse is insignificant for the DW motion because it creates the paramagnetic-like state before switched domains are nucleated. We note that there should be an optimal pulse interval between the two pulses in the dual-pulse switching processes, as observed in Fig. 4. When the pulse interval is too short, the domains return to the paramagnetic-like state because the spin temperature rises again to T_C . On the other hand, when the pulse interval is too long, the recovered magnetic properties slow down the DW motion. Therefore, to move the DW efficiently, the spin temperature should be as close to T_C as possible but must stay below T_C .

In the case of the single-pulse excitation, the laser pulse has basically passed through the system before the magnetization reaches its minimum [23] and switched domains nucleate. Understandably, a heat gradient across a DW never forms unless a switched domain already exists. Even when switched domains already exist, the single-pulse excitation is inefficient

because the reduction of the magnetization and the formation of the heat gradient across a DW develop simultaneously.

In conclusion, we have demonstrated that our dual-pulse method can drastically reduce the pulse number required for AO-HDS in a Pt/Co/Pt structure. Using a linearly polarized femtosecond pulse for the first pump and a circularly polarized picosecond pulse for the second pump, we successfully realized a record small number of 8 pulses to fully switch a magnetic domain. Dual-pulse AO-HDS proceeds through two stages: helicity-independent creation of switched domains and helicity-dependent DW motions, where the pulse interval between the two pulses and the pulse width of the second circularly polarized pulse are crucial. This result suggests that the dual-pulse method is a potential route towards realizing very efficient AO-HDS in ferromagnetic metals.

ACKNOWLEDGMENTS

We thank T. Toonen and C. Berkhout for the continuous technical supports and T. Taniguchi for the valuable comments on sample fabrication. This work was partly supported by the European Research Council Grant Agreement No. 339813 (Exchange), the FOM programme Exciting Exchange, de Nederlandse Organisatie voor Wetenschappelijk Onderzoek (NWO), the EU H2020 Program Grant Agreement No. 713481 (SPICE), spintronic-photonic integrated circuit platform for novel electronics, and Grants-in-Aid for Specially Promoted Research from JSPS No. 15H05702.

- [1] S. Manipatruni, and D. E. Nikonov, I. A. Young, *Nat. Phys.* **14**, 338-343 (2018).
- [2] A. Brataas, A. D. Kent, and H. Ohno, *Nat. Mater.* **11**, 372-381 (2012).
- [3] A. Kirilyuk, A. V. Kimel, and Th. Rasing. *Rev. Mod. Phys.* **82**, 2731-2784 (2010).

- [4] C. D. Stanciu, F. Hansteen, A. V. Kimel, A. Kirilyuk, A. Tsukamoto, A. Itoh, and Th. Rasing, *Phys. Rev. Lett.* **99**, 047601 (2007).
- [5] T. A. Ostler, J. Barker, R. F. L. Evans, R. W. Chantrell, U. Atxitia, O. Chubykalo-Fesenko, S. El Moussaoui, L. Le Guyader, E. Mengotti, L. J. Heyderman, F. Nolting, A. Tsukamoto, A. Itoh, D. Afanasiev, B. A. Ivanov, A. M. Kalashnikova, K. Vahaplar, J. Mentink, A. Kirilyuk, Th. Rasing, and A. V. Kimel, *Nat. Commun.* **3**, 666 (2012).
- [6] A. R. Khorsand, M. Savoini, A. Kirilyuk, A. V. Kimel, A. Tsukamoto, A. Itoh, and Th. Rasing, *Phys. Rev. Lett.* **108**, 127205 (2012).
- [7] C-H. Lambert, S. Mangin, B. S. D. Ch. S. Varaprasad, Y. K. Takahashi, M. Hehn, M. Cinchetti, G. Malinowski, K. Hono, Y. Fainman, M. Aeschlimann, and E. E. Fullerton, *Science* **345**, 1337-1340 (2014).
- [8] M. S. El Hadri, P. Pirro, C.-H. Lambert, S. Petit-Watelot, Y. Quessab, M. Hehn, F. Montaigne, G. Malinowski, and S. Mangin, *Phys. Rev. B* **94**, 064412 (2016).
- [9] M. S. El Hadri, M. Hehn, P. Pirro, C.-H. Lambert, G. Malinowski, E. E. Fullerton, and S. Mangin, *Phys. Rev. B* **94**, 064419 (2016).
- [10] R. Medapalli, D. Afanasiev, D. K. Kim, Y. Quessab, S. Manna, S. A. Montoya, A. Kirilyuk, Th. Rasing, A. V. Kimel, and E. E. Fullerton, *Phys. Rev. B* **96**, 224421 (2017).
- [11] Y. Quessab, R. Medapalli, M. S. El Hadri, M. Hehn, G. Malinowski, E. E. Fullerton, S. Mangin, *Phys. Rev. B* **97**, 054419 (2018).
- [12] U. Parlak, R. Adam, D. E. Bürgler, S. Gang, and C. M. Schneider, *Phys. Rev. B* **98**, 214443 (2018).
- [13] R. John, M. Berritta, D. Hinzke, C. Müller, T. Santos, H. Ulrichs, P. Nieves, J. Walowski, R. Mondal, O. Chubykalo-Fesenko, J. McCord, P. M. Oppeneer, U. Nowak, and M. Münzenberg, *Sci. Rep.* **7**, 4114 (2017).

- [14] See Supplemental Material for the magnetization curve, the illustration of the optical imaging set-up, the spot size determination, checking the reversibility and pulse width dependence of dual-pulse AO-HDS, and the ultrafast demagnetization of the Pt/Co/Pt structure.
- [15] J. M. Liu, *Opt. Lett.* **7**, 196-198 (1982).
- [16] M. Berritta, R. Mondal, K. Carva, and P. M. Oppeneer, *Phys. Rev. Lett.* **117**, 137203 (2016).
- [17] R. Knorren, K. H. Bennemann, R. Burgermeister, and M. Aeschlimann, *Phys. Rev. B* **61**, 9427 (2000).
- [18] J. R. Rumble, (ed.) CRC Handbook of Chemistry and Physics, 99th edn (CRC Press, Boca Raton, 2017).
- [19] K. Uchida, T. Ota, K. Harii, S. Takahashi, S. Maekawa, Y. Fujikawa, and E. Saitoh, *Solid State Commun.* **150**, 524 (2010).
- [20] M. Hatami, G. E. W. Bauer, Q. Zhang, and P. J. Kelly, *Phys. Rev. Lett.* **99**, 066603 (2007).
- [21] H. Yu, S. Granville, D. P. Yu, and J.-Ph. Ansermet, *Phys. Rev. Lett.* **104**, 146601 (2010).
- [22] D. Hinzke, and U. Nowak, *Phys. Rev. Lett.* **107**, 027205 (2011).
- [23] A. Foghini, G. Salvatella, R. Gort, T. Michlmayr, A. Vaterlaus, and Y. Acremann, *Struct. Dyn.* **2**, 024501 (2015).
- [24] E. Beaurepaire, J.-C. Merle, A. Daunois, and J.-Y. Bigot, *Phys. Rev. Lett.* **76**, 4250-4253 (1996).
- [25] B. Koopmans, G. Malinowski, F. Dalla Longa, D. Steiauf, M. Fähnle, T. Roth, M. Cinchetti, and M. Aeschlimann, *Nat. Mater.* **9** 259-265 (2010).
- [26] P. Tengdin, W. You, C. Chen, X. Shi, D. Zusin, Y. Zhang, C. Gentry, A. Blonsky, M. Keller, P. M. Oppeneer, H. C. Kapteyn, Z. Tao, and M. M. Murnane, *Sci. Adv.* **4**, 977 (2018).

[27] W. You, P. Tengdin, C. Chen, X. Shi, D. Zusin, Y. Zhang, C. Gentry, A. Blonsky, M. Keller, P. M. Oppeneer, H. Kapteyn, and Z. Tao, *Phys. Rev. Lett.* **121**, 077204 (2018).

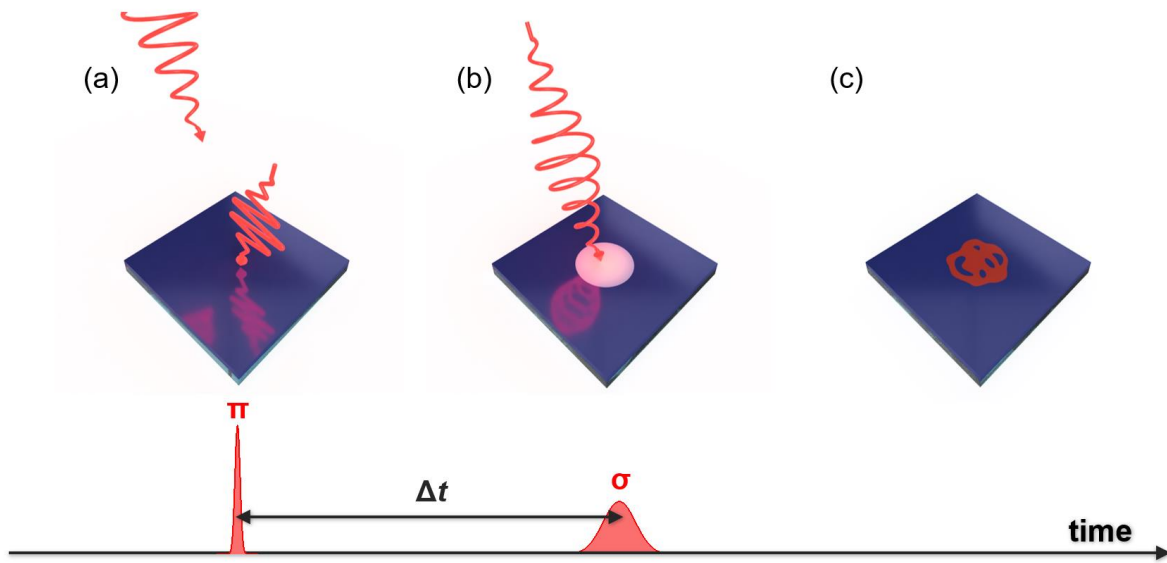


FIG. 1. (a)-(c) Principal concept of dual-pulse all-optical helicity-dependent switching (AO-HDS). (a) A short linearly polarized (π) pulse arrives at the down-magnetized system and decreases the magnetic properties, resulting in reduction in the energy barrier for the magnetization switching. (b) The longer circularly polarized (σ) pulse reaches the film after a constant pulse interval (Δt), and induces helicity-dependent effects to switch the magnetization. In this case, an up-magnetized state is anticipated as the final state, as depicted in (c).

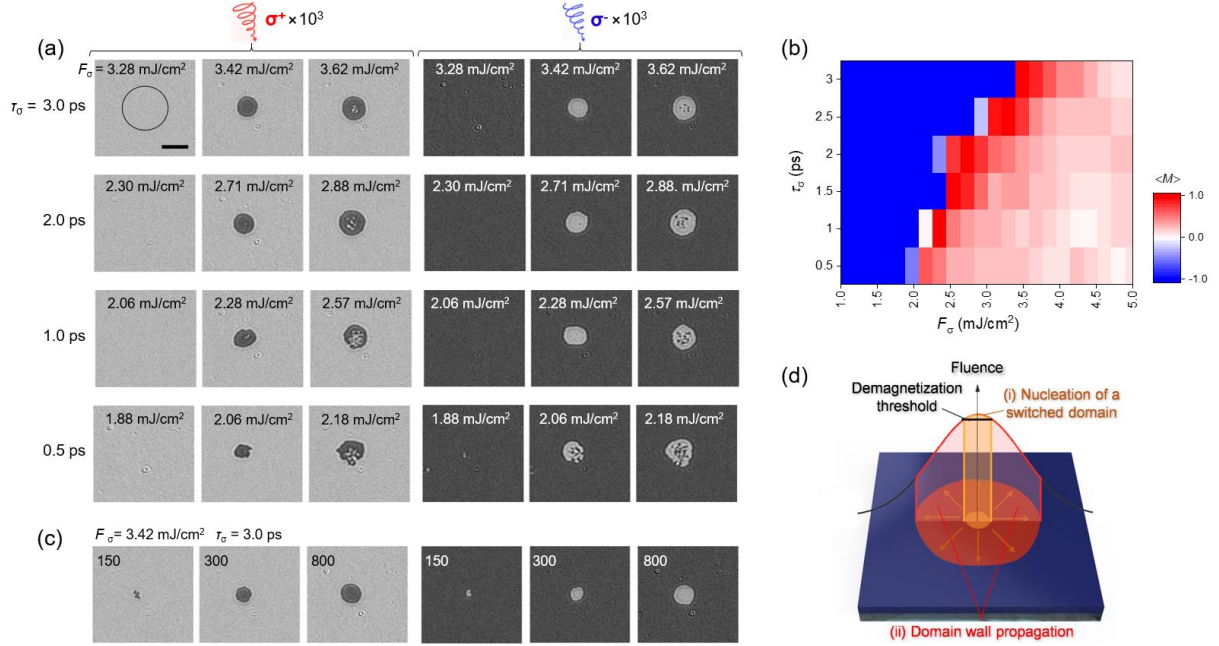


FIG. 2. (a) AO-HDS by multiple pulses of circularly polarized laser with the pulse width (τ_σ) in the range of 0.5 -3.0 ps. Each magneto-optical image was taken after illuminating the uniformly magnetized film with 1,000 pulses of right (σ^+) or left (σ^-) circular polarization with a constant fluence (F_σ) at a laser repetition rate of 1 kHz. The darker (brighter) area denotes up (down)-magnetization. A continuous-line circle indicates the size of the focused circularly polarized pulse (52.0 ± 0.8 μm in diameter). The scale bar corresponds to 30 μm . (b) Averaged net magnetization $\langle M \rangle$ after 1,000 circularly polarized pulses plotted as function of τ_σ and F_σ . $\langle M \rangle = -1$ means that the magnetic state of a 15- μm diameter area is the same as the initial one, and $\langle M \rangle$ reaches 1 when the magnetic state is uniformly switched. (c) Magneto-optical images after illumination with 150, 300, and 800 circularly polarized pulses. Here, the value of F_σ was fixed at 3.42 mJ/m². (d) Schematic illustration of the switching process of multi-pulse AO-HDS. When the central fluence of the Gaussian laser spot goes above the demagnetization threshold, a switched domain nucleates at the spot center. Then, the DW concentrically propagates driven by circularly polarized pulses.

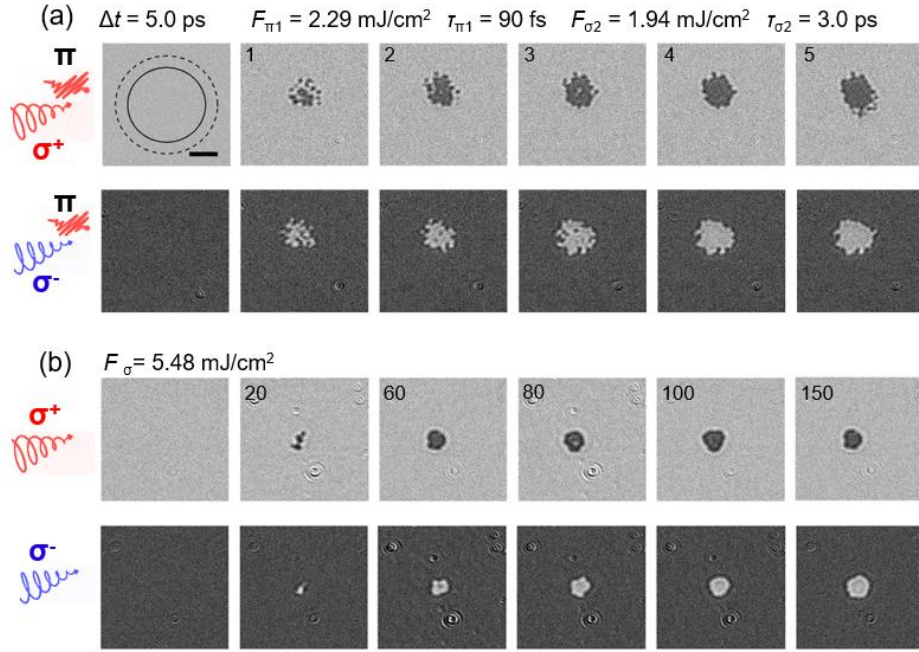


FIG. 3. (a) AO-HDS with a combination of short linearly and long circularly polarized pulses. We used a 90-fs linearly polarized laser pulse with fluence ($F_{\pi 1}$) of 2.29 mJ/cm^2 as the first pump pulse. A 3-ps circularly polarized pulse with fluence ($F_{\sigma 2}$) of 1.94 mJ/cm^2 reaches the sample after a pulse interval (Δt) of 5.0 ps. (b) Multi-pulse AO-HDS for comparison. The images were taken after illumination with circularly polarized pulses with $F_{\sigma} = 5.48 \text{ mJ/cm}^2$, where the pulse interval was set to be at least 1 second to compare the two cases. The numbers of (pairs of) pulses are shown in the snapshots. The sizes of the circularly and linearly polarized pulses are indicated by continuous- and broken-line circles, 68.2 ± 1.8 and $52.0 \pm 0.8 \mu\text{m}$ in diameter, respectively. The scale bar corresponds to $20 \mu\text{m}$.

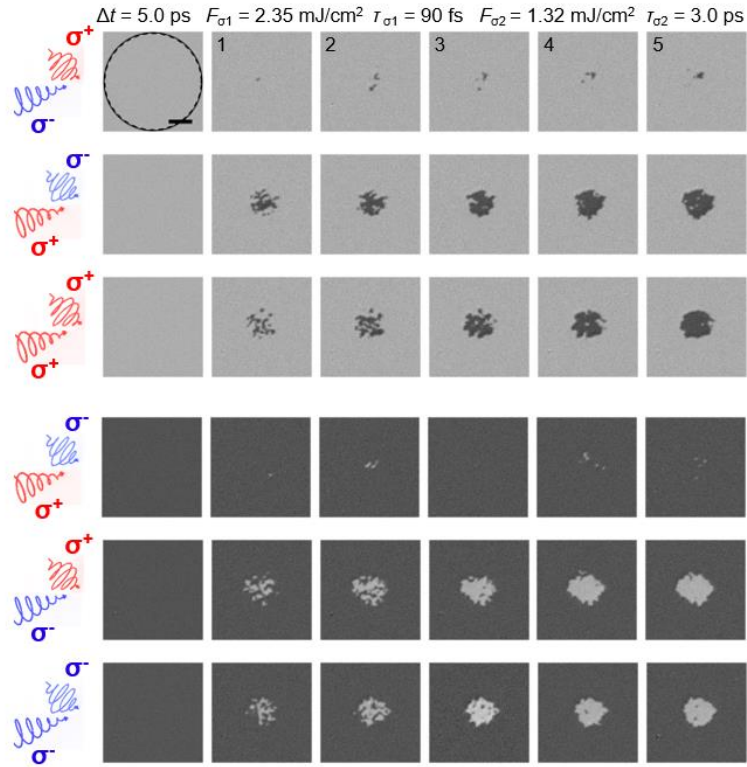


FIG. 4. AO-HDS with a combination of short and long circularly polarized pulses. Snapshots before and after illuminating the uniformly magnetized sample with 1-5 pairs of pulses with the pulse interval Δt of 5.0 ps are displayed. Here, we used a 90-fs circularly polarized laser pulse with fluence (F_{σ_1}) of 2.35 mJ/cm² and 3-ps circularly polarized laser pulse with fluence (F_{σ_2}) of 1.32 mJ/cm². The continuous- and broken-line circles denote the spot sizes of the short and long pulses of 84.2 ± 1.2 and 82.7 ± 1.0 μm in diameter, respectively. The scale bar is 20 μm .

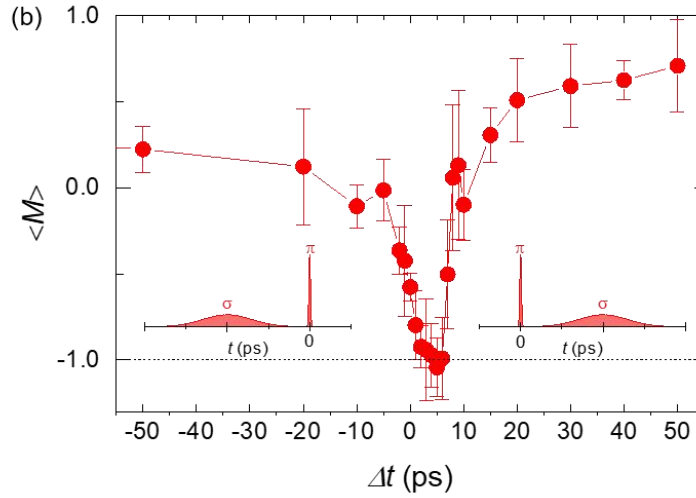
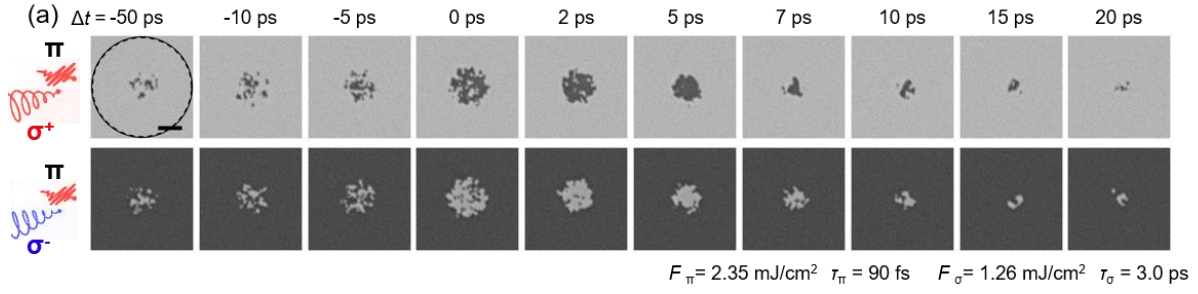


FIG. 5. (a) Pulse interval (Δt) dependence of dual-pulse AO-HDS. Snapshots after 4 pairs of pulses at positive and negative Δt are shown. Here, we used a 90-fs linearly polarized laser pulse with fluence (F_{π}) of 2.35 mJ/cm² and 3-ps circularly polarized laser pulse with fluence (F_{σ}) of 1.26 mJ/cm². Positive (Negative) Δt means that the linearly polarized pulse arrives at the film earlier (later) than the circularly polarized pulse. The spot sizes of the circularly (continuous-line circle) and linearly polarized (broken-line circle) pulses are 84.2 ± 1.2 and 82.7 ± 1.0 μm in diameter, respectively. The scale bar corresponds to 20 μm . (b) Averaged net magnetization $\langle M \rangle$ after 4 pairs of pulses as a function of Δt . $\langle M \rangle = -1$, 0, and +1 correspond to initial uniformly-magnetized, demagnetized, and fully-switched states of a 15- μm diameter area, respectively.